Appl. Phys. B 34, 123–128 (1984)

Applied Physics B Photophysics and Laser Chemistry

Analysis of Temporal Pulse Development in Passively Mode-Locked Lasers

F. Graf, G. Pleininger, and A. Penzkofer

Naturwissenschaftliche Fakultät II – Physik, Universität, D-8400 Regensburg, Fed. Rep. Germany

Received 5 March 1984/Accepted 31 March 1984

Abstract. Pulse-shortening and pulse broadening effects in passively mode-locked lasers are analysed. A steady-state pulse duration limit is calculated and compared with round-trip simulations. The numerical calculations apply to a picosecond Nd : glass laser. Methods of short-pulse generation are discussed.

PACS: 42.55R, 42.60D, 42.65

In passively mode-locked pulsed lasers the statistical spontaneous emission bursts have a duration approximately equal to the inverse of the fluorescence linewidth. In the linear laser phase (constant dye absorption) the finite spectral gain profile of the active medium narrows the spectral width and broadens the duration of the circulating spikes. In the nonlinear laser phase (nonlinear dye transmission, mode-locking region) the most intense spike is preferentially amplified and strong background discrimination is achieved. Pulse shortening occurs in the saturable absorber cell. (For reviews on mode-locking see [1–7].) The natural mode selection in the active medium acts against the shortening. Intensity dependent loss mechanisms like two-photon absorption in Nd: glass rods [8] broaden the pulse duration at high laser intensities [9].

In this paper we analyse the pulse shortening and pulse broadening effects in passively mode-locked lasers. Intensity-dependent stationary pulse durations are found by equating pulse shortening and pulse broadening per round-trip in the laser oscillator. In the mode-locking region the transient temporal development of a picosecond pulse with constant background level is simulated and the approach to the stationary situation is studied.

The theory presented applies to all passively mode-locked lasers, either pulsed or continuously working [10]. The numerical calculations in this paper apply to a passively mode-locked Nd:glass laser. The calculations reveal conditions for optimum short-pulse generation in the oscillator. Preliminary measurements with a Pockels cell intensity limiter in the resonator led to pulse shortening in agreement with the theory.

1. Stationary Pulse Durations

The changes of pulse duration per round-trip in the oscillator are analysed. Pulses are broadened by the finite spectral width of the gain and by intensity dependent nonlinear losses. Here pulse broadening by two-photon absorption in Nd : glass rods is discussed. Pulse shortening occurs in the nonlinear transmission region of the saturable absorber.

The pulse duration ratio $\beta = \Delta t_{L,0}/\Delta t_{L,i}$, where $\Delta t_{L,0}$ is the pulse duration after $n+1$ round-trips and $\Delta t_{L,i}$ the pulse duration after n round-trips, is given by

$$\beta = \beta_{\mathrm{GAIN}} \beta_{\mathrm{TPA}} \beta_{\mathrm{DYE}} . \tag{1}$$

β_{GAIN} is the ratio of pulse broadening by the finite spectral width of the gain profile. β_{TPA} represents the ratio of pulse broadening by two-photon absorption in the active medium. β_{DYE} is the pulse shortening ratio of the saturable dye.

The spectral gain profile of the active medium approximately has the form [9]

$$g(\nu - \nu_0) = G(\nu)/G(\nu_0) \tag{2}$$

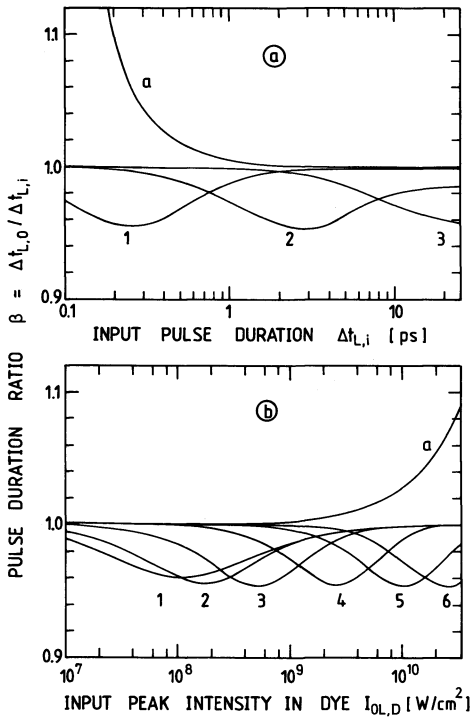

Fig. 1a and b. Pulse duration changes per round-trip in the oscillator. Curves are calculated with parameters of Table 1. (a) Curve *a*, pulse broadening due to finite spectral gain width β_{GAIN}. Curves *1–3*, pulse shortening in saturable dye β_{DYE} for *(1)* $I_{OL,D}=10^{10}$ W/cm², *(2)* 10^9 W/cm², and *(3)* 10^8 W/cm². (b) Curve *a*, pulse broadening due to two-photon absorption β_{TPA}. Curves *1–6*, pulse shortening in dye β_{DYE} for *(1)* $\Delta t_{L,i}=500$ ps (steady state), *(2)* 20 ps, *(3)* 5 ps, *(4)* 1 ps, *(5)* 0.25 ps, and *(6)* 0.1 ps

Table 1. Parameters used in calculations

Resonator

Configuration:	hemi-confocal
Mirror reflectivities:	$R_1=0.3$, $R_2=0.997$
Linear transmission:	$T_l=0.9$
Focusing ratio:	$\kappa=I_{0L,D}/I_{0L,A}=6.5$

Active Medium

Type: Nd-phosphate glass LG 703 from Glaswerke Schott	
Fluorescence halfwidth	$\Delta\nu_G=189\,\mathrm{cm}^{-1}$ (FWHM)
Spectral gain width	$\Delta\nu_g=163\,\mathrm{cm}^{-1}$ (FWHM) [9]
Pumped length	$l_A=10$ cm
Rod length	$l_R=13$ cm
Stimulated emission cross-section	$\sigma_A=4.1\times10^{-20}$ cm²
Two-photon absorption coefficient	$\alpha^{(2)}=4\times10^{-12}$ cm/W

Saturable Absorber

Type: Kodak No. 9860	
Absorption recovery time	$\tau_D=7$ ps [16]
Absorption cross-section	$\sigma_D=3.7\times10^{-16}$ cm²
Excited state absorption cross-section	$\sigma_{ex}=0$ (assumed)
Single pass small signal transmission	$T_0=0.85$

Stationary Conditions

Pulse shape: Gaussian

Transient Start Conditions (End of Linear Phase)

Pulse shape	$s(t)=(1-\beta)\exp(-t^2/t_0^2)+\beta$
Duration	$\Delta t=t_0/[2(\ln2)^{1/2}]=9$ ps, $t_0=5.4$ ps
Background to peak intensity ratio	$\beta=I_B/I_{0L,1}=1/7$
Peak intensity	$I_{0L,D,1}=10^6$ W/cm²
Net gain	$G_N=1.03$
Saturation factor	$\delta=0.98$

with the gain factors

$$G(\nu)=\exp\{2l_A\sigma_A N_i\exp[-(\nu-\nu_0)^2/\nu_G^2]\} \tag{3}$$

and

$$G(\nu_0)=\exp(2l_A\sigma_A N_i)\simeq\frac{G_N}{R_1R_2T_lT_0^2}; \tag{4}$$

l_A is the length of the active medium, σ_A is the stimulated emission cross-section. $N_i=N_{2,A}-N_{1,A}$ represents the number density of inverted active ions that emit at frequency ν_0. A Gaussian spectral emission shape is assumed with an 1/e width of ν_G. G_N is the net gain per round-trip at the end of the linear phase. R_1 and R_2 are the mirror reflectivities. T_l accounts for linear losses and T_0 is the small signal single-pass transmission of the saturable dye. The full halfwidth of the gain profile $g(\nu-\nu_0)$ is $\Delta\nu_g$ [found by setting $g(\nu-\nu_0)=1/2$]. The temporal response function corresponding to the spectral gain profile $g(\nu-\nu_0)$ is approximately of Gaussian shape and has a full halfwidth of $\Delta t_g=0.44/\Delta\nu_g$. The temporal pulse broadening per round-trip is given by the convolution of the pulse shape with the response function. In our calculations the broadening ratio is approximated by

$$\beta_{GAIN}=\frac{(\Delta t_{L,i}^2+\Delta t_g^2)^{1/2}}{\Delta t_{L,i}}. \tag{5}$$

In Fig. 1a the curve *a* shows the dependence of β_{GAIN} on $\Delta t_{L,i}$ for a Nd-phosphate glass oscillator with the laser parameters listed in Table 1. The steep rise of β_{GAIN} when $\Delta t_{L,i}$ approaches $\Delta\nu_g^{-1}$ sets a lower limit to the obtainable pulse duration. The halfwidth of the gain profile $\Delta\nu_g$ is slightly smaller than the halfwidth of the fluorescence profile $\Delta\nu_G=2[\ln(2)]^{1/2}\nu_G$. A reasonable estimate of β_{GAIN} is already obtained by using $\Delta\nu_G$ instead of $\Delta\nu_g$.

Intensity dependent losses broaden bell-shaped light pulses. Two-photon absorption is observed in Nd:glass lasers [8]. The two-photon intensity transmission per round-trip is

$$T_{TPA}=\frac{1}{1+\alpha^{(2)}2l_RI_{0L,A,i}\exp(-t^2/t_0^2)}; \tag{6}$$

$\alpha^{(2)}$ is the two-photon absorption cross-section. l_R is the laser rod length and $I_{0L,A,i}$ is the pulse peak intensity in the laser rod. $t_0 = \Delta t_{L,i}/[2(\ln 2)^{1/2}]$ is the 1/e temporal pulse width. A Gaussian temporal pulse shape is assumed. The spatially averaged two-photon power transmission $\bar{T}_{TPA}$ is found approximately by using an average intensity $\bar{I}_{0L,A,i} = 0.5 \times I_{0L,A,i}$. The temporal broadening β_{TPA} is found by calculating the halfwidth $\Delta t_{L,0}$ of the transmitted pulse of intensity distribution $I_{L,A,0}(t) = \bar{T}_{TPA} I_{L,A,i}(t)$ and forming the ratio $\beta_{TPA} = \Delta t_{L,0}/\Delta t_{L,i}$. The result is

$$\beta_{TPA} = \frac{[\ln 2 + \ln(1 + 0.5\alpha^{(2)} l_R I_{0L,A,i})]^{1/2}}{(\ln 2)^{1/2}}. \quad (7)$$

The curve *a* of Fig. 1b represents the dependence of the broadening factor β_{TPA} on input peak intensity $I_{0L,D}$ in the saturable absorber for the parameters listed in Table 1. A ratio of $\kappa = I_{0L,D}/I_{0L,A} = 6.5$ is used in the calculations. The ratio applies to a hemiconfocal resonator with contacted dye cell at the plane mirror (used in the experiments) [10]. With increasing pulse intensity the temporal pulse broadening due to two-photon absorption rises strongly. The pulse broadening depends on the temporal pulse shape. Only rectangularly shaped pulses ($I_L(t) = I_{0L}[\theta(t) - \theta(t - \Delta t_L)]$; $\theta(\zeta < 0) = 0$, $\theta(\zeta > 0) = 1$) are not broadened by two-photon absorption (constant intensity causes constant loss).

The pulse shortening in the saturable dye is described here by a special model of isotropic interaction of light with a four-level system: The laser light excites dye molecules from the S_0-ground state (1) to a Franck-Condon level in the S_1 state (2). From there the molecules relax infinitely fast to a temporal equilibrium position (3) in the S_1 state from where the molecules decay to the ground state (1). Excited state absorption from level (3) to a higher lying state (4) with infinitely fast relaxation is included. This model leads to the equation system

$$\frac{\partial N_{3,D}}{\partial t} = \frac{I_{L,D}(t)}{h\nu_L} \sigma_D (N_{0,D} - N_{3,D}) - \frac{N_{3,D}}{\tau_D}, \quad (8)$$

$$\frac{\partial I_L}{\partial z} = -I_L \sigma_D (N_{0,D} - N_{3,D}) - I_L \sigma_{ex} N_{3,D}. \quad (9)$$

$N_{0,D} = N_{1,D} + N_{3,D}$ is the total number density of dye molecules. σ_D is the ground-state absorption cross-section. σ_{ex} denotes the excited state absorption. τ_D is the absorption recovery time. The initial conditions are $N_{3,D}(t = -\infty, z) = 0$ and $I_{L,D}(t, z = 0) = I_{0L,D} \exp(-t^2/t_0^2)$. The isotropic calculations for spatial rectangular pulses, (8) and (9), give about the same result for energy transmission and pulse shortening as anisotropic calculations for spatial Gaussian pulses.

The shortening of Gaussian light pulses by passing through the contacted saturable absorber cell is depicted in Fig. 1a and b. The parameters used in the calculations belong to the mode-locking dye Kodak No. 9860 (Table 1). The Curves *1–3* in Fig. 1a present β_{DYE} versus $\Delta t_{L,i}$ for fixed values of $I_{0L,D}$ while the Curves *1–6* in Fig. 1b belong to $\beta_{DYE}(I_{0L,D})$ for various input pulse durations $\Delta t_{L,i}$.

The saturable absorber has an optimum intensity region of efficient pulse shortening. This optimum intensity region starts approximately at the saturation intensity $I_S = h\nu_L/(\sigma_D \tau_D)$ for pulses of long duration (steady state situation) and shifts to higher intensity values with decreasing input pulse duration. The minimum shortening ratio $\beta_{DYE,min}$ is nearly independent of the ratio $\tau_D/\Delta t_{L,i}$. The pulse shortening ratio is increased with decreasing initial dye transmission T_0. Excited state absorption reduces the pulse shortening effect somewhat. The pulse shortening ratio is also dependent on the pulse shape [11].

More refined models of saturable absorption are described in [12, 13]. The pulse shortening behaviour of the more complex models is the same. Additional pulse shortening by transient gratings formed in the contacted dye cell [14, 15] is not included in our analysis.

A stationary pulse duration is achieved if the pulse broadening effects are exactly compensated by the pulse shortening effects, i.e. $\beta = \beta_{GAIN}\beta_{TPA}\beta_{DYE} = 1$. Figure 2 presents two equilibrium curves in the $(\Delta t_L, I_{0L,D})$-plane. The solid curve belongs to the parameters of Fig. 1 listed in Table 1 ($T_0 = 0.85$, Gaussian pulse shape, $\alpha^{(2)} = 4 \times 10^{-12}$ cm/W, $\sigma_{ex} = 0$). The curve indicates a minimum steady state pulse duration of 0.38 ps at $I_{0L,D} \simeq 5 \times 10^9$ W/cm^2. It divides the plane into the two regions *I* and *II*. Transient pulse durations in region *I* are shortened until the lower branch of the solid curve is reached. Initial pulses in region *II* are elongated. In region *IIa* the temporal broadening stops when the solid curve is reached (stable equilibrium). In region *IIb* the pulses continuously broaden. The upper branch of the solid curve represents an unstable equilibrium.

Saturable absorbers with excited state absorption have a slightly reduced pulse shortening effect. For $\sigma_{ex} = 1 \times 10^{-16}$ cm^2 and all other parameters the same as for the presented solid curve the minimum possible pulse duration becomes $\Delta t_{L,min} \simeq 0.47$ ps at $I_{0L,D} \simeq 4 \times 10^9$ W/cm^2. The use of higher concentrated saturable dyes shifts the equilibrium curve to lower pulse durations. A small signal dye transmission of $T_0 = 0.70$ ($\sigma_{ex} = 0$) leads to $\Delta t_{L,min} \simeq 0.23$ ps at $I_{0L,D} \simeq 7 \times 10^9$ W/cm^2. Calculating the equilibrium

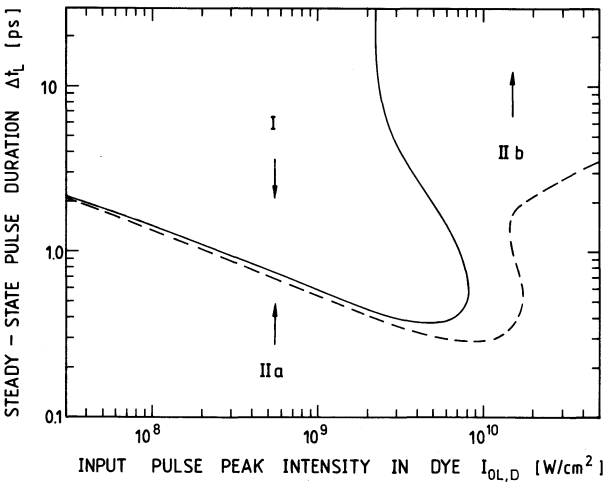

Fig. 2. Stationary equilibrium pulse duration versus pulse intensity. Solid curve represents data of Table 1. The dashed curve is calculated for $\alpha^{(2)}=0$. The other parameters are the same as for the solid curve. Pulses in region *I* are shortened, in region *II* are broadened

curve for the saturable absorber No. 5 (from Kodak or Lambda Physik) with the parameters $\sigma_D=3\times10^{-16}$ cm^2, $\tau_D=2.7$ ps [16] and $\sigma_{ex}=0$ (assumed) leads to practically the same result as for the dye Kodak No. 9860. Despite the negligible differences in the stationary equilibrium behaviour, the transient pulse development in real pulsed mode-locked lasers is different for mode-locking dye No. 5 and No. 9860 [17, 18].

The dashed curve in Fig. 2 is calculated without two-photon absorption. The other parameters are the same as for the solid curve (Table 1). A minimum stationary pulse duration of $\Delta t_{L,\min}\simeq0.3$ ps is achieved at $I_{0L,D}\simeq10^{10}$ W/cm^2. Initial pulses below the curve are elongated while initial pulses above the curve are shortened. For absorption recovery times τ_D longer than the stationary equilibrium duration $\Delta t_L(I_{0L,D})$ the bleaching and pulse shortening becomes nearly independent of τ_D [19] and the stationary equilibrium curve $\Delta t_L(I_{0L,D})$ (dashed curve) remains unchanged. In this case the bleaching behaviour is determined by the saturation energy $E_S=h\nu_L/\sigma_D$. Large absorption cross-sections shift the equilibrium pulse duration curve to lower intensity values.

2. Transient Pulse Development

The above discussion about the stationary pulse duration does not indicate how fast the equilibrium is approached. To study the transient behaviour we simulated the pulse development in the nonlinear laser region [9].

At the jth round trip in the nonlinear phase the intensity distribution $I_{L,j}(t)$ changes to

$$I_{L,j+1}(\beta_{\text{GAIN},j}t)=I_{L,j}(t)G_jR_1R_2T_lT_{D,j}(t)T_{\text{TPA},j}(t). \quad (10)$$

The temporal broadening due to the gain medium is taken into account by rescaling the time axis after each round-trip from $t_j=t$ to $t_{j+1}=\beta_{\text{GAIN},j}t$. The light amplification in the active medium is

$$G_j=\frac{1+(G_N-1)\delta}{R_1R_2T_lT_0^2}. \quad (11)$$

The net gain per round-trip at the end of the linear phase is set to $G_N=1.03$ in the presented calculations. The factor $\delta\leqq1$ takes into account gain depletion due to reduction of inversion ($\delta=0.98$ used in calculations). The double-pass pulse transmission through the contacted dye cell $T_D(t)=I_{L,\text{out}}(t)/I_{L,\text{in}}(t)$ (in linear region $T_D=T_0^2$) is calculated by solving (8) and (9) [9]. The two-photon transmission $T_{\text{TPA},j}(t)$ is given by (6).

The calculations start at the end of the linear phase with an initial pulse intensity

$$I_{L,1}(t)=I_{0L,1}[\exp(-4\ln2t^2/\Delta t_0^2)(1-\beta)+\beta]. \quad (12)$$

Equation (12) approximates the real intensity distribution by the most intense spike with peak intensity $I_{0L,1}$ and a constant background level $I_B=\beta I_{0L,1}$. The background intensity I_B is set equal to the mean spike intensity $\langle I\rangle$ in the resonator which is given by $\langle I\rangle=\beta I_{0L,1}\approx I_{0L,1}/\ln(2m)$, where $m=T/(2\Delta t_0)$ is the number of pulses within the resonator round-trip time $T=2L/c$ (L resonator length, $L=1.5$ m in our case) [6].

In Fig. 3 numerical results for a mode-locked Nd : glass laser with saturable dye Kodak No. 9860 are presented (parameters in Table 1). The initial pulse parameters are taken from theoretical studies of the prelaser and linear laser phase [20] and are experimentally verified by measuring the spectral width of the free-running laser (without saturable absorber). After a certain intensity level is reached the laser intensity is kept constant for further round-trips as is indicated in Fig. 3a. The calculated pulse durations versus the number of round-trips in the nonlinear phase are shown in Fig. 3b. For the constant intensity region the Curves *1–3* start in region *I* of Fig. 2 and pulse shortening is achieved. About 200 round-trips are necessary to approach the steady state equilibrium. The constant intensity values of Curves *4* and *5* ($I_{0L,D}=6.5\times10^9$ W/cm^2 and 2.6×10^{10} W/cm^2) lie in region *IIb* and the pulses are gradually elongated. The steady state limits *1′–3′* expected from Fig. 2 are not reached since the evolving temporal pulse profile deviates from Gaussian shape.

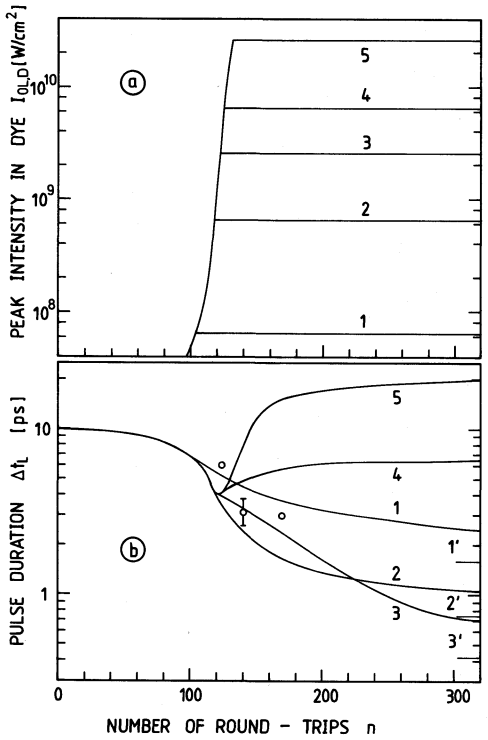

Fig. 3a and b. Pulse development in mode-locking region of the laser. (a) Development of the peak pulse intensity. (b) Corresponding pulse durations. Parameters of Table 1 are used in the calculations. Experimental points belong to pulses limited to $I_{0L,D} \simeq 3 \times 10^{10}$ W/cm² with an intracavity Pockels cell. They should follow Curve *3* (stationary intensity $I_{0L,D} = 2.6 \times 10^{9}$ W/cm²)

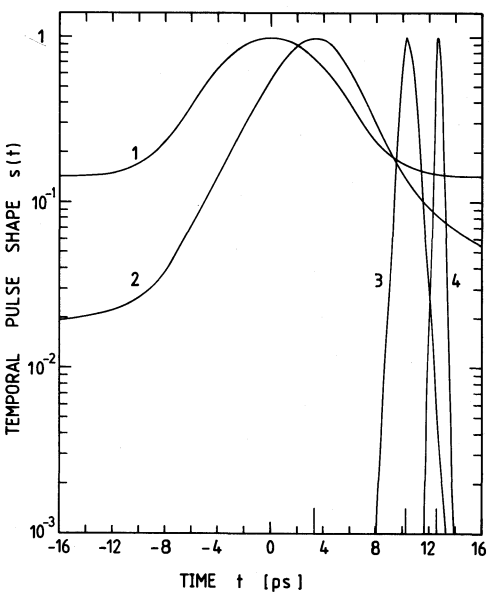

Fig. 4. Temporal pulse shape along the pulse train. Curve *(1)*, shape at end of linear phase, *(2)* after 100, *(3)* 200, and *(4)* 300 round-trips in nonlinear phase. Curves belong to pulse development depicted by Curve *2* in Fig. 3 (stationary intensity $I_{0L,D} = 6.5 \times 10^{8}$ W/cm²) and data of Table 1

The approached stationary pulse duration is independent of the initial pulse duration. In the transient mode-locking region of the laser, shorter starting pulses result in shorter final pulse durations [9, 21–24] if the net gain per round-trip is high enough that the initial pulse does not die out and only the trailing background signal survives. (Curves *2* and *2'* in [9, Fig. 4] are correct for $G_N \simeq 1.05$. For $G_N = 1.03$ the initial pulse is absorbed and the background signal at the trailing edge of the pulse forms a pulse with duration longer than Curves *1* and *1'* of the same picture.)

Figure 4 shows the temporal pulse shape at the beginning of the mode-locking region, after 100, 200, and 300 round-trips for Curve *2* of Fig. 3. An asymmetric shape is formed due to the finite absorption recovery time and the background signal. The calculated pulse asymmetry is in agreement with experimental findings [25, 26].

3. Prospects of Short Pulse Generation

In conventional passively mode-locked lasers the optimum intensity region of efficient pulse shortening is passed too fast (Fig. 3a) and the minimum possible pulse duration is not achieved. The obtained peak intensity in the pulse train maximum can only be slightly influenced by mirror reflectivity. The region of pulse broadening by two-photon absorption is reached in mode-locked Nd : glass lasers. The intensity region of optimum pulse shortening in the absorber may be brought to the region of maximum peak pulse intensity by changing the resonator configuration and appropriate positioning the absorber cell in the resonator (influence of factor $\kappa = I_{0L,D}/I_{0L,A}$) or by applying a lens system in the resonator. Positioning the dye cell to a low intensity position in the resonator makes it difficult to start the mode-locking process since then even the most intense laser spike of the linear laser region does not reach the mode-locking threshold [20]. The use of two dye cells at different positions overcomes this problem as was checked experimentally.

Another possibility of pulse shortening is to fix the laser intensity in the resonator to the optimum pulse shortening region with an intensity limiter. In preliminary experiments we inserted a dielectric polarizer and a Pockels cell into the oscillator. With a photodiode triggered krytron system the Pockels cell was operated [27] when the laser intensity approached a value of $I_{0L,D}$ around 3×10^{9} W/cm². The voltage to the Pockels cell was regulated in such a way that the gain per round-trip became equal to the loss at the polarizer. The circulating pulse intensity remained

approximately constant over up to fifty round-trips. The intensity limitation by the Pockels cell and polarizer does not cause a pulse broadening as intensity limitation by two-photon absorption does [28]. The pulse duration could be shortened from 6 to 3 ps. The experimental points are included in Fig. 3. They should follow the theoretical Curve *3* which was calculated for $I_{0L,D}=2.6\times10^9$ W/cm^2. The agreement between the experimental points and the calculated curve is fairly good.

4. Conclusions

The temporal pulse development in passively mode-locked lasers was studied. The numerical examples were restricted to a pulsed passively mode-locked Nd:glass lasers but the theoretical considerations apply as well to other passively mode-locked laser systems. Without external manipulations the optimum intensity region for efficient pulse shortening is passed too fast and high intensity values are approached, where nonlinear loss mechanisms broaden the pulse duration. The insertion of a Pockels cell intensity limiter opens the possibility of optimum pulse shortening in the laser oscillator.

Acknowledgements. The authors are indepted to Prof. W. Kaiser for valuable discussions. They thank Th. Ascherl for technical assistance, P. Sperber for some investigations of lasers with two dye cells, and the Rechenzentrum of this University for disposal of computer time.

References

1. A.J. DeMaria, W.H. Glenn, M.J. Brienza, M.E. Mack: Proc. IEEE **57**, 2 (1969)
2. P.G. Kryukov, V.S. Letokhov: IEEE J. QE-**8**, 766 (1972)
3. D. von der Linde: Appl. Phys. **2**, 281 (1973)
4. A. Laubereau, W. Kaiser: Opto-Electronics **6**, 1 (1974)
5. D.J. Bradley: In *Ultrashort Light Pulses*, ed. by S.L. Shapiro, Topics Appl. Phys. **18** (Springer, Berlin, Heidelberg, New York 1977) p. 17
6. W.H. Lowdermilk: In *Laser Handbook*, Vol. III, ed. by M.L. Stitch (North-Holland, Amsterdam 1979) p. 361
7. M.S. Demokan, Mode-Locking: In *Solid-State and Semiconductor Lasers* (Research Studies Press, Chichester 1982)
8. A. Penzkofer, W. Kaiser: Appl. Phys. Lett. **21**, 547 (1972)
9. F. Graf, C. Löw, A. Penzkofer: Opt. Commun. **47**, 329 (1983)
10. J. Herrman, F. Weidner, B. Wilhelmi: Appl. Phys. B **26**, 197 (1981)
11. A. Penzkofer: Opto-Electronics **6**, 87 (1974)
12. A. Penzkofer, W. Blau: Opt. Quantum Electron. **15**, 325 (1983)
13. W. Blau, R. Reber, A. Penzkofer: Opt. Commun. **43**, 210 (1983)
14. D. Kühlke, W. Rudolph, B. Wilhelmi: IEEE J. QE-**19**, 526 (1983)
15. D. Kühlke, W. Rudolph: Opt. Quantum Electron **16**, 57 (1984)
16. B. Kopainsky, W. Kaiser, K.H. Drexhage: Opt. Commun. **32**, 451 (1980)
17. C. Kolmeder, W. Zinth: Appl. Phys. **24**, 341 (1981)
18. R.R. Alfano, N.H. Schiller, G.A. Reynolds: IEEE J. QE-**17**, 290 (1981)
19. G. Grönninger, A. Penzkofer: Opt. Quantum Electron. (1984, to be published)
20. A. Penzkofer: To be published
21. M.W. McGeoch: Opt. Commun. **7**, 116 (1973)
22. D. von der Linde, K.F. Rodgers: Opt. Commun. **8**, 91 (1973)
23. E.M. Gordeev, P.G. Kryukov, Yu.A. Matveets, B.M. Stepanov, S.D. Fachenko, S.V. Chekalin, A.V. Sharkov: Sov. J. Quantum Electron. **5**, 129 (1975)
24. H. Graener, A. Laubereau: Opt. Commun. **37**, 138 (1981)
25. J. Wiedmann, A. Penzkofer: Opt. Commun. **30**, 107 (1979)
26. W. Leupacher, A. Penzkofer: Appl. Phys. B **29**, 263 (1982)
27. J. Biebl, A. Penzkofer: J. Phys. E **13**, 1328 (1980)
28. J.M. Ralston, R.K. Chang: Appl. Phys. Lett. **15**, 164 (1969)